

Electrical Properties of the n-NiS₂/n-CdTe Isotype Heterojunction Fabricated by Spray Pyrolysis

I.G. ORLETSKYI, M.I. ILASHCHUK, E.V. MAISTRUK,
I.P. KOZIARSKYI* AND D.P. KOZIARSKYI

Department of Electronics and Power Engineering, Yuriy Fedkovych Chernivtsi National University, Kotsubynsky st. 2, 58002 Chernivtsi, Ukraine

Doi: [10.12693/APhysPolA.142.615](https://doi.org/10.12693/APhysPolA.142.615)

*e-mail: i.koziarskyi@chnu.edu.ua

The conditions for the fabrication of n-NiS₂/n-CdTe isotype heterojunctions with diode properties by spray pyrolysis of n-NiS₂ thin films on n-CdTe crystalline substrates have been studied. The temperature dependence of the current–voltage characteristics is analyzed, and the mechanisms of the current generation at the heterojunction at forward and reverse voltages are determined. Based on the analysis of the capacitance–voltage characteristics, a model of a double Schottky diode for the studied heterojunction is presented, which well describes the observed electrophysical phenomena.

topics: NiS₂, spray pyrolysis, heterojunction, energy diagram

1. Introduction

Recently, much attention has been paid to nanostructured transition metal sulfides due to their unique optical, electrical, magnetic, and catalytic properties [1]. The properties of these materials largely depend on the dimensions, volumes, methods, and modes of manufacture [2, 3]. Transition metal sulfides are promising for use in supercapacitors [4], lithium-ion batteries [5], hydrogen evolution reactions [6], and solar cells [7–10].

Nickel sulfides stand out for their low cost, non-toxicity, and chemical stability among transition metal sulfides. Nickel with sulfur forms numerous phases, such as NiS, NiS₂, Ni₃S₂, Ni₃S₄, Ni₇S₆, and Ni₉S₈, suitable for various applications. Nickel disulfide NiS₂ has a band gap $E_g \approx 1.3$ eV [11, 12], which is in the optimal energy range for photoelectric energy conversion [13]. Nickel sulfide films are prepared using hydrothermal [12] and solvothermal methods [14], decomposition of precursors [15], microwave-assisted synthesis [16], spray pyrolysis [17], and others.

Cadmium telluride with a band gap $E_g = 1.5$ eV and a high absorption coefficient $\alpha = 10^5$ cm⁻¹ is successfully used in photovoltaics. Heterojunctions with films of transition metal sulfide MnS and FeS₂ were fabricated on CdTe substrates by an inexpensive spray pyrolysis method [18, 19]. The use of a semiconductor solid solution CdSe_xTe_{1-x} ($0.3 < x < 0.4$) with a band gap $E_g \approx 1.4$ eV in the design of solar cells based on cadmium telluride was one of the factors in obtaining energy conversion efficiency of more than 22% [20]. This inspired the study of the pyrolysis spray fabrication conditions

and the physical properties of the NiS₂ semiconductor heterocontact with $E_g \approx 1.3$ eV (lower than that of CdSeTe) with cadmium telluride, which is presented in this paper.

2. Experimental details

CdTe plates with a thickness of $d \approx 1$ mm and a surface area of $S \approx 3 \times 4$ mm² were used to fabricate the n-NiS₂/n-CdTe isotype heterojunction by spray pyrolysis. The substrates were obtained by cleavage from crystalline ingots grown by the vertical Bridgman method. CdTe samples had electronic conductivity. Their specific conductivity was $\sigma = 3.3$ Ω⁻¹ cm⁻¹, electron concentration $n = 2.7 \times 10^{16}$ cm⁻³, and Hall mobility was $\mu_H = 760$ cm² V⁻¹ s⁻¹ at a temperature of 300 K.

When fabricating n-NiS₂/n-CdTe heterojunctions, n-NiS₂ films (thickness $\simeq 0.17$ μm) were deposited on freshly chipped n-CdTe substrates by spray pyrolysis. The pyrolysis temperature was $T_S = 350^\circ\text{C}$. A pneumatic sprayer was used to obtain an aerosol of salt solutions. Aerosol solutions were prepared by dissolving NiCl₂ · 2H₂O and (NH₂)₂CS salts in double-distilled water. The 0.1 M solution was mixed with the 0.1 M (NH₂)₂CS solution in a volume ratio (at which [S]/[Ni] = 2) before aerosol formation. Stirring for three hours at room temperature with a magnetic stirrer was carried out to homogenize the resulting mixture. The solution was heated to a temperature of $\simeq 70^\circ\text{C}$, and a few drops of hydrochloric acid were added after stirring. The solution was clear and remained stable for several days.

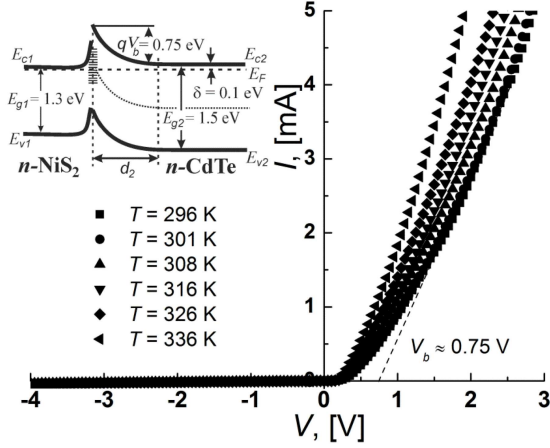


Fig. 1. I - V -characteristics of the n-NiS₂/n-CdTe heterojunction at temperatures from 296 K to 336 K and energy diagram of the heterojunction (inset).

In addition to CdTe substrates, in the preparation of n-NiS₂ films, in one technological process, soda-lime glass (for the study of optical properties) and crystalline glass-ceramic (for the study of electrical properties of films) substrates were used. The optical band gap of the films was $E_g \approx 1.3$ eV according to the study of the transmission spectra of nickel disulfide films on glass and the calculation of the absorption coefficient. The resistivity of n-NiS₂ films (which are made on the sital) was quite low $\rho \approx 1.7 \times 10^{-4}$ Ω cm according to studies by the four-probe method. External contacts of the n-NiS₂/n-CdTe structure on the side of low-resistance n-NiS₂ films were fabricated using silver-based conductive paste, and on the side of n-type CdTe substrates — by melting indium. The current-voltage (I - V) characteristics of n-NiS₂/n-CdTe heterojunctions at different temperatures were measured on a setup using Shch300 and V7-16A devices. The stability of the electrical properties of the n-NiS₂/n-CdTe heterojunctions was controlled by an L2-56 curve tracer. The measurements of capacitance-voltage (C - V) characteristics of structures in a wide range of frequencies of the measurement signal were carried out by an LCR Meter BR2876.

3. Results and discussion

I - V -characteristics of n-NiS₂/n-CdTe heterojunctions measured at temperatures from $T = 293$ K to $T = 336$ K are shown in Fig. 1. Forward bias of the heterojunction, at which there is a sharp increase in current, is observed at a positive potential on the n-NiS₂ film. This indicates that a built-in electric field formed by the positive charge of donors in the n-CdTe near-contact region is present in the fabricated structure.

The current rectification ratio was 2×10^2 (at $|V| = 1$ V) at $T = 297$ K in the fabricated n-NiS₂/n-CdTe heterojunctions. The voltage φ_k (cor-

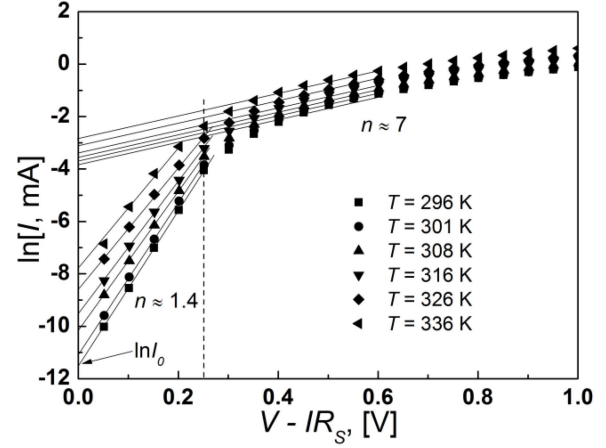


Fig. 2. Temperature dependences $\ln I = f(V - IR_S)$ at forward voltage at the n-NiS₂/n-CdTe heterojunction.

responding to a rapid increase in forward current) was estimated by extrapolation to the voltage axis of the linear sections of the I - V -characteristic at forward bias. The voltage φ_k makes it possible to estimate, in the first approximation, the value of the potential built into the heterojunction $V_b \approx 0.75$ V (at $T = 296$ K).

The forward branches of the I - V -characteristics in the coordinates $\ln(I) = f(V)$ were used to determine the methods of forming forward currents through the n-NiS₂/n-CdTe heterojunction. The dependencies $\ln(I) = f(VIR_S)$ (Fig. 2) were constructed in order to avoid affecting the results of the analysis of the current generation mechanisms of the series resistance (which in the n-NiS₂/n-CdTe structure is $R_S \approx 300$ Ω).

The slope of the linear dependencies $\ln(I) = f(V)$ corresponds to the value of the diode coefficient $n \approx 1.4$ at forward voltages $3k_B T/q < V < 0.25$ V. The slope $\ln(I) = f(V)$ decreases with increasing temperature, which indicates the over-barrier mechanism of current flow, which is described by the formula [21]

$$I = I_0 \exp\left(\frac{qV}{nk_B T}\right), \quad (1)$$

where n is the diode coefficient, and I_0 is given by

$$I_0 = A^{**} T^2 \exp\left(-\frac{qV_b}{k_B T}\right), \quad (2)$$

where A^{**} is the Richardson constant, and qV_b is the height of the potential barrier at the electrical junction.

It was found that $\ln(I_0)$ determines the height of the potential barrier qV_b at the n-NiS₂/n-CdTe isotype heterojunction. Note that $\ln(I_0)$ at each temperature T was found by extrapolation of the dependencies $\ln(I) = f(V)$ (with diode coefficient $n = 1.4$) to the $\ln I$ axis. The value $qV_b = 0.75$ eV was obtained from the tangent of the angle of inclination of the dependence

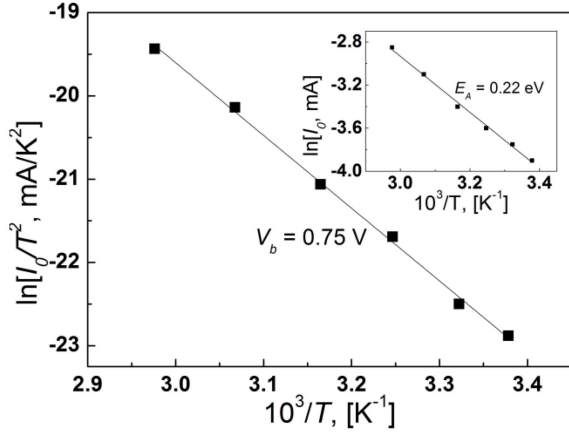


Fig. 3. Determination of the height of the potential barrier qV_b at the n-NiS₂/n-CdTe heterojunction from the dependence $\ln(I_0/T^2) = f(10^3/T)$ and the activation energy E_A of the forward tunneling current (inset).

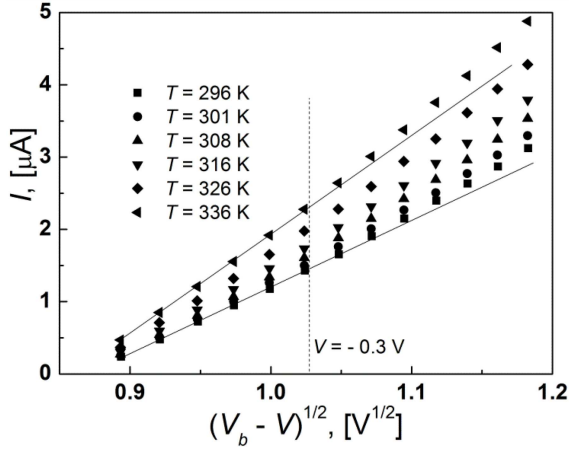


Fig. 4. Linear temperature dependences of the reverse I - V -characteristics for the n-NiS₂/n-CdTe heterojunction at voltages of $-0.3 \text{ V} < V < -3k_B T/q$.

$\ln(I_0/T^2) = f(10^3/T)$ (Fig. 3) according to (2). The value of qV_b correlates well with the value of the contact potential difference V_b (estimated from forward I - V -characteristics (Fig. 1)).

Diode coefficient is $n \approx 7$ at forward voltages $0.25 \text{ V} < V < 0.7 \text{ V}$. In this case, the absence of the temperature dependence of the tangent of the angle of inclination $\ln(I) = f(V)$ indicates the tunneling mechanism of forward current, which for isotype junction is described by the expression [22]

$$I(V) = I_0 \exp(\alpha(V_b - V)), \quad (3)$$

where $I_0 = B \exp(E_A/k_B T)$, B and α are constants, and E_A is the activation energy of the tunneling current.

The activation energy of the forward tunneling current at the n-NiS₂/n-CdTe heterojunction was determined according to (3) from the tangent of

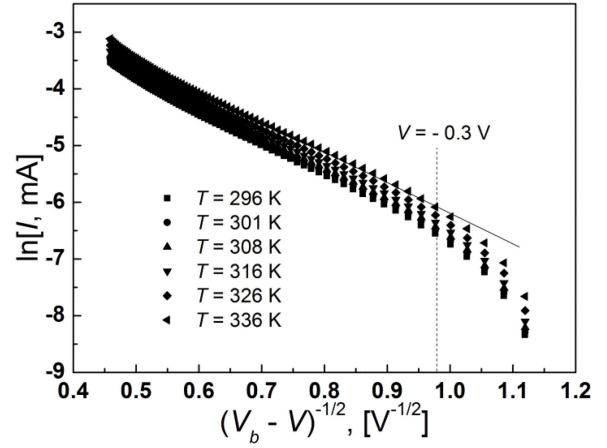


Fig. 5. Linear temperature dependences of the reverse I - V -characteristics of the n-NiS₂/n-CdTe heterojunction in the voltage range $-3 \text{ V} < V < -0.3 \text{ V}$.

the angle of inclination of the dependence $\ln(I_0) = f(10^3/T)$ in the voltage range $0.25 \text{ V} < V < 0.7 \text{ V}$ and was $E_A = 0.22 \text{ eV}$. The obtained value agrees well with Fig. 2, in which the transition from the over-barrier current to the tunneling current occurs at forward biases $V \approx 0.25 \text{ V}$ (when the electron energy in n-CdTe increases by 0.25 eV). The thickness of the barrier at the n-NiS₂/n-CdTe heterojunction, as estimated from capacitance measurements at zero bias, is about 800 nm , which indicates the impossibility of direct electron tunneling from the n-CdTe conduction band to the n-NiS₂ conduction band. With such a barrier thickness, the tunneling mechanism is implemented with the participation of energy states in the band gap in the near-contact region on the n-CdTe side (multistage tunneling).

The voltage dependence of the reverse current for the n-NiS₂/n-CdTe heterojunction indicates the generation mechanism of current generation at reverse biases in the range $-0.3 \text{ V} < V < -3k_B T/q$ [23]

$$I = \frac{qn_i d_2}{\tau} = \frac{n_i}{\tau} \sqrt{\frac{2q}{N_d}} (V_b - V), \quad (4)$$

where n_i is the intrinsic concentration of charge carriers in n-CdTe, d_2 is the thickness of the electron-depletion region in n-CdTe, τ is the lifetime of charge carriers in the depletion region, and N_d is the donor concentration.

The I - V -characteristic is linear in the coordinates $I = f((V_b - V)^{1/2})$ (Fig. 4) at reverse biases $-0.3 \text{ V} < V < -3k_B T/q$, according to (4). Charge carriers are generated in the depletion n-CdTe region of the heterojunction.

The reverse current is formed by the transfer of a negative charge of electrons in the conduction band to the bulk part of the n-CdTe region and the movement of the positive charge of holes to the heterojunction boundary and their recombination with

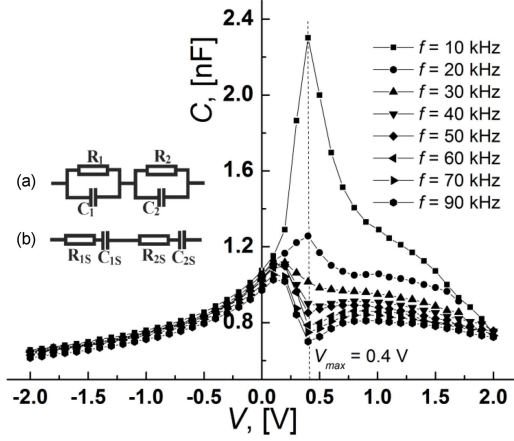


Fig. 6. C - V -characteristics of the n-NiS₂/n-CdTe heterojunction in the measuring signal frequency range from 10 kHz $< f < 100$ kHz and equivalent parallel (b) and series (c) circuits (inset).

the electrons of the conduction band of the n-NiS₂ film with the participation of states in the band gap at the heterojunction boundary.

The I - V -characteristic of the n-NiS₂/n-CdTe heterojunction at reverse voltages $V < -0.3$ V is described by the expression for the tunneling current [22]

$$I = a_0 \exp\left(-b_0 (V_b - V)^{-1/2}\right), \quad (5)$$

where a_0 is a parameter that depends on the probability of filling the energy levels from which electron tunneling occurs, and b_0 is determined by the dynamics of current change from voltage.

The I - V -characteristic of the n-NiS₂/n-CdTe heterojunction in the coordinates $\ln(I) = f((V_b - V)^{-1/2})$ according to (5) is linear (Fig. 5).

The C - V -characteristics of the n-NiS₂/n-CdTe heterojunction in the measuring signal frequency ranges from 10 kHz to 100 kHz (Fig. 6) and 200 kHz $< f < 1000$ kHz (Fig. 7) have a form that is typical for isotype heterojunctions formed by participation of a negative charge energy states at the semiconductor interface. In this case, the Schottky double diode model [24] is used to analyze the properties. In this model, the heterojunction is represented as two diodes that are connected to each other. The energy diagram of the n-NiS₂/n-CdTe heterojunction based on this model is shown in the insert in Fig. 1. The C - V -characteristics of the heterojunction are determined by the ratio of the series-connected capacitors C_1 of the depletion region on the n-NiS₂ side, and C_2 of the depletion region on the n-CdTe side.

The equivalent parallel circuit of the n-NiS₂/n-CdTe heterojunction, which also contains differential resistances of the electrical junction R_1 and R_2 (in addition to capacitors C_1 and C_2) is shown in Fig. 6, inset a, and a series circuit is shown in Fig. 6, inset b. The connection of these equivalent circuits

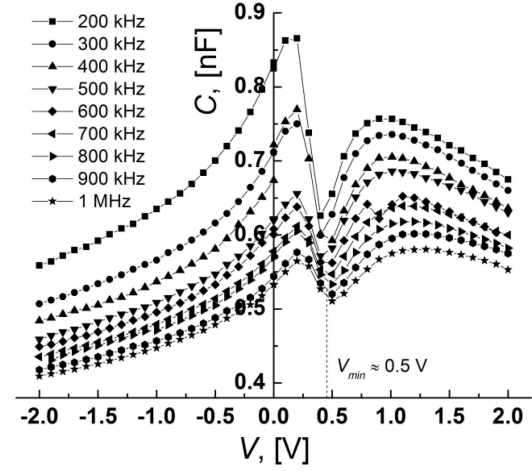


Fig. 7. C - V -characteristics of the n-NiS₂/n-CdTe heterojunction at frequencies 200 kHz $< f < 1$ MHz.

makes it possible to establish the dependence of capacitances and differential resistances on the frequency ω of the measuring signal [25]

$$C_{1S} = \frac{C_1 (1 + (\omega\tau_1)^2)}{(\omega\tau_1)^2}, \quad (6)$$

$$C_{2S} = \frac{C_2 (1 + (\omega\tau_2)^2)}{(\omega\tau_2)^2}, \quad (7)$$

$$R_{1S} = \frac{R_1}{1 + (\omega\tau_1)^2}, \quad (8)$$

$$R_{2S} = \frac{R_2}{1 + (\omega\tau_2)^2}, \quad (9)$$

where $\tau_1 = R_1 C_1$, $\tau_2 = R_2 C_2$.

The differential resistance $R_2 \gg R_1$ and capacitance C_1 at reverse biases of the n-NiS₂/n-CdTe heterojunction (positive potential at n-CdTe) are shunted. The variable signal is applied to C_2 , and the capacitance of the heterojunction is determined by the capacitance $C = C_2$. With forward biases, R_1 increases and R_2 decreases. The variable signal is fully applied to C_1 , and the total capacitance $C = C_1$ at a frequency $f = 10$ kHz at a forward voltage $V \approx 0.4$ V, $R_2 \ll R_1$. The switching voltage of the variable signal to measure the capacitance C_1 decreases with increasing frequency of the measuring signal since it occurs at higher differential resistance, which for the variable signal is small enough due to a decrease with frequency (according to (7)). The capacitance in the voltage range 0.25 V $< V < 0.5$ V is determined by the capacitance of the depletion region in the n-NiS₂ film for frequencies $f = 200$ – 1000 kHz (Fig. 7). The total capacitance C decreases as the electrical junction in n-NiS₂ is reverse-biased and expands with forward voltage applied to the n-NiS₂/n-CdTe structure.

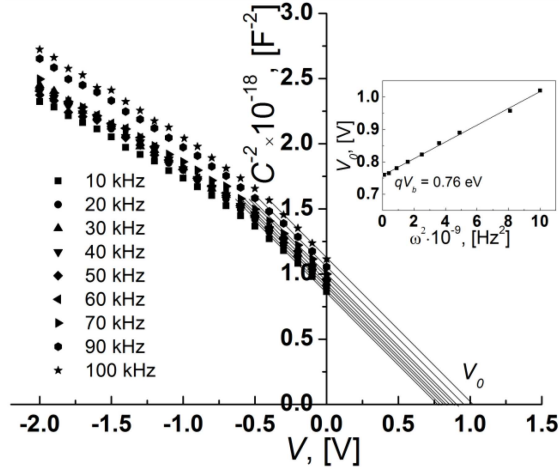


Fig. 8. Dependence $C^{-2} = f(V)$ for n-NiS₂/n-CdTe heterojunction at frequencies $10 \text{ kHz} < f < 100 \text{ kHz}$ and dependence $V_0 = f(\omega^2)$ (inset).

The capacitance of the n-NiS₂/n-CdTe heterojunction is determined by the capacitance of the electron-depletion region in n-CdTe at negative voltages. The dependences $1/C^2 = f(V)$ in the range of reverse voltages when the frequency changes from 10 to 100 kHz are characterized by a shift in the characteristics $1/C^2 = f(V)$ along the y -axis (Fig. 8) due to the effect of series resistance R_S . The total capacitance C , according to the Goodman model [26], is described by the expression

$$C^{-2} = C_0^{-2} + 2\omega^2 R_S^2, \quad (10)$$

where C_0 is the capacitance of the charge carriers depletion region.

The values of V_0 were found by extrapolation to the voltage axis of the linear dependences $1/C_2 = f(V)$ at different frequencies to determine the contact potential difference V_b according to C - V -characteristics (Fig. 8). The dependence $V_0 = f(\omega^2)$ was constructed (Fig. 8, inset), which at $\omega^2 = 0$ indicates the value of the contact potential difference $V_b \approx 0.76 \text{ V}$.

The obtained value agrees well with the value $V_b \approx 0.75 \text{ V}$, obtained according to the methods shown in Figs. 1 and 3.

Two linear regions are observed for the dependences $1/C^2 = f(V)$ at reverse voltage, which correspond to different concentrations N_{D1} and N_{D2} of the electrically active donor impurity in n-CdTe. The rate of change in the capacitance of the heterojunction from the voltage at voltages from $V = 0 \text{ V}$ to $V \approx -0.6 \text{ V}$ is higher than the rate of change in capacitance at $V < -0.6 \text{ V}$. The impurity concentrations N_{D2} in the near-contact region of the heterojunction and N_{D1} in the depth of the n-CdTe base region are determined by the expressions [27]

$$\tan(\alpha_1) = \frac{2}{q\varepsilon_S\varepsilon_0 N_{D1} S^2}, \quad (11)$$

$$\tan(\alpha_2) = \frac{2}{q\varepsilon_S\varepsilon_0 N_{D2} S^2}, \quad (12)$$

where q is the electron charge, $S = 9 \text{ mm}^2$ is the electrical junction area, $\varepsilon_S = 10$ is the relative permittivity of the semiconductor, $\varepsilon_0 = 8.85 \times 10^{-12} \text{ F/m}$ — electric constant. The calculated values of donor concentration are $N_{D1} = 2.62 \times 10^{16} \text{ cm}^{-3}$ and $N_{D2} = 1.57 \times 10^{16} \text{ cm}^{-3}$. A region with a lower N_D concentration is formed in n-CdTe on the side of contact with the n-NiS₂ film due to cadmium atom vacancies that appear during the fabrication of the heterojunction.

4. Conclusions

The n-NiS₂/n-CdTe isotype heterojunction with a rectification ratio of $\approx 10^2$ was fabricated by spray pyrolysis of a mixture of 0.1 M aqueous solutions of NiCl₂ · 2H₂O and (NH₂)₂CS salts at the temperature of n-CdTe substrates $T_S = 350^\circ\text{C}$. The diode properties of the heterojunction are determined by the energy barrier $\approx 0.75 \text{ eV}$, which is formed in the near-contact region of n-CdTe. The over-barrier current flows in the heterojunction at a forward bias of up to 0.25 V. The current is formed by tunneling electrons from the n-CdTe conduction band to the n-NiS₂ conduction band with the participation of energy states in the band gap at $V > 0.4 \text{ V}$. The reverse current in the voltage range $-0.3 \text{ V} < V < -3k_B T/q \text{ V}$ is formed as a result of the thermal generation of charge carriers in the depletion region of n-CdTe. Tunneling of electrons through the barrier with the participation of energy states in the n-CdTe band gap, which are localized in the near-contact region of the heterojunction, predominates with increasing reverse voltage ($-3 \text{ V} < V < -0.3 \text{ V}$). The C - V -characteristics of the n-NiS₂/n-CdTe heterojunction are described by the model of a double Schottky diode based on the dynamics of changes in the properties of two electrical junctions upon application of an external voltage.

References

- [1] W. Zhu, Y. Cheng, C. Wang, N. Pinna, X. Lu, *Nanoscale* **13**, 9112 (2021).
- [2] M.M. Gomaa, M.H. Sayed, M.S. Abdel-Wahed, M. Boshta, *RSC Adv.* **12**, 10401 (2022).
- [3] J.S. Anand, R.K.M. Rajan, A.A.M. Zaidan, *Rep. Electrochem.* **3**, 25 (2013).
- [4] L. Peng, X. Ji, H. Wan, Y. Ruan, K. Xu, C. Chen, L. Miao, J. Jiang, *Electrochimica Acta* **182**, 361 (2015).
- [5] J. Zhao, Y. Zhang, Y. Wang, H. Li, Y. Peng, *J. Energy Chem.* **27**, 1536 (2018).

- [6] Q. Ma, C. Hu, K. Liu, S.-F. Hung, D. Ou, H.M. Chen, G. Fu, N. Zheng, *Nano Energy* **41**, 148 (2017).
- [7] F. Li, J. Wang, L. Zheng, Y. Zhao, N. Huang, P. Sun, L. Fang, L. Wang, X. Sun, *J. Power Sources* **384**, 1 (2018).
- [8] X. Cao, R. Ding, Y. Zhang, Y. Cui, K. Hong, *M. Today Commun.* **26**, 102160 (2021).
- [9] Z. Wan, C. Jia, Y. Wang, *Nanoscale* **7**, 12737 (2015).
- [10] X. Zuo, S. Yan, B. Yang, G. Li, M. Wu, Y. Ma, S. Jin, K. Zhu, *J. Mater. Sci. Mater. Electron.* **27**, 7974 (2016).
- [11] Y. Liu, X. Hao, H. Hu, Z. Jin, *Acta Phys.-Chim. Sin.* **37**, 2008030 (2021).
- [12] A.M. Huerta-Flores, L.M. Torres-Martínez, E. Moctezuma, A.P. Singh, B. Wickman, *J. Mater. Sci. Mater. Electron.* **29**, 11613 (2018).
- [13] A.L. Fahrenbruch, R.H. Bube, *Fundamentals of Solar Cells* Academic Press, 1983.
- [14] X. Yang, L. Zhou, A. Feng, H. Tang, H. Zhang, Z. Ding, Y. Ma, M. Wu, S. Jin, G. Li, *J. Mater. Res.* **29**, 935 (2014).
- [15] C. Buchmaier, M. Glänzer, A. Torvisco, P. Poelt, K. Wewerka, B. Kunert, K. Gatterer, G. Trimmel, T. Rath, *J. Mater. Sci.* **52**, 10898 (2017).
- [16] M. Lu, N. Gao, X.-J. Zhang, G.-S. Wang, *RSC Adv.* **9**, 5550 (2019).
- [17] D. Mondal, G. Villemure, G. Li, C. Song, J. Zhang, R. Hui, J. Chen, C. Fairbridge, *Appl. Catal. A General* **450**, 230 (2013).
- [18] I.G. Orletskyi, M.I. Ilashchuk, E.V. Maistruk, H.P. Parkhomenko, P.D. Maryanchuk, I.P. Kozziarskyi, D.P. Kozziarskyi, *Mater. Res. Express* **8**, 015905 (2021).
- [19] I.G. Orletskyi, M.I. Ilashchuk, M.N. Solovan, P.D. Maryanchuk, O.A. Parfenyuk, E.V. Maistruk, S.V. Nichyi, *Semiconductors* **52**, 1171 (2018).
- [20] A. Romeo, E. Artegiani, *Energies* **14**, 1684 (2021).
- [21] E.H. Rhoderick, *Metal — Semiconductor Contacts* Clarendon Press, Oxford, 1978.
- [22] B.L. Sharma, R.K. Purohit, *Semiconductor Heterojunctions* Pergamon Press, 1974.
- [23] S.M. Sze, K.N. Kwok, *Physics of Semiconductor Devices*, Wiley, 2006.
- [24] C. van Opdorp, H.K.J. Kanerva, *Solid State Electron.* **10**, 401 (1967).
- [25] V.V. Brus, *Semicond. Sci. Technol.* **27**, 035024 (2012).
- [26] A.M. Goodman, *J. Appl. Phys.* **34**, 329 (1963).
- [27] I.G. Orletskyi, M.I. Ilashchuk, M.M. Solovan, P.D. Maryanchuk, E.V. Maistruk, G.O. Andrushchak, *Mater. Res. Express* **6**, 086219 (2019).